Preparation and Functional Evaluation of RGD-Modified Proteins as $\alpha_v\beta_3$ Integrin Directed Therapeutics

Robbert J. Kok,*,§ Astrid J. Schraa,‡,§ Erwin J. Bos, Henk E. Moorlag,‡ Sigridur A. Ásgeirsdóttir,§ Maaike Everts,§ Dirk K. F. Meijer, and Grietje Molema†

Groningen University Institute for Drug Exploration (GUIDE), Department of Pharmacokinetics and Drug Delivery, University Centre for Pharmacy, A. Deusinglaan 1, 9713 AV Groningen, The Netherlands. Received October 3, 2001; Revised Manuscript Received November 16, 2001

Tumor blood vessels can be selectively targeted by RGD-peptides that bind to $\alpha_v\beta_3$ integrin on angiogenic endothelial cells. By inhibiting the binding of these integrins to its natural ligands, RGD-peptides can serve as antiangiogenic therapeutics. We have prepared multivalent derivatives of the cyclic RGD-peptide c(RGDfK) by covalent attachment of the peptide to side chain amino groups of a protein. These RGDpep−protein conjugates inhibited $\alpha_v\beta_3$-mediated endothelial cell adhesion in vitro, while conjugates prepared with a control RAD-peptide showed no activity. Radiobinding and displacement studies with endothelial cells demonstrated an increased affinity of the RGDpep−protein conjugates compared to the free peptide, with IC_{50} values ranging from 23 to 0.6 nM, depending on the amount of coupled RGDpep per protein. Compared to the parental RGD-peptide and the related RGD-peptide ligand c(RGDfV), the RGDpep−protein conjugates showed a considerable increase in affinity (IC_{50} parent RGDpep: 818 nM; IC_{50} c(RGDfV): 158 nM). We conclude that the conjugation of RGD-peptides to a protein, resulting in products that can bind multivalently, is a powerful approach to increase the affinity of peptide ligands for $\alpha_v\beta_3/\alpha_v\beta_5$ integrins.

INTRODUCTION

The formation of new blood vessels is essential for the supply of oxygen and nutrients to proliferating tumor cells. Antitumor therapies that aim at the endothelium of these newly formed tumor blood vessels seem attractive for several reasons. First, the disruption of one blood vessel will result in the killing of a multitude of tumor cells, as shown by inhibiting angiogenesis or by inducing tumor vasculature selective blood coagulation (*1*). Second, endothelial cells of tumor blood vessels are normal, nontransformed cells and therefore less likely to become resistant to antitumor therapy than tumor cells. Last, the endothelium lining the blood vessels is easily accessible for systemically applied therapeutics.

Newly formed blood vessels are characterized by the expression of surface molecules that are not present on resting endothelium (*2*). One of these so-called angiogenic markers is the $\alpha_v\beta_3$ integrin. Cyclic peptides containing a conformationally restrained Arg-Gly-Asp (RGD) sequence have been developed as ligands for $\alpha_v\beta_3$ and the closely related $\alpha_v\beta_5$ integrin (*3*). For instance, the dicyclic peptide CDCRGDCFC (RGD-4C)[1] has been used as a targeting moiety to selectively deliver doxorubicin to angiogenic blood vessels (*4*). A drawback of the RGD-4C peptide is the instability of the two disulfide bridges that maintain the specific three-dimensional structure of the peptide (*5*). A chemically more stable peptide with high affinity for $\alpha_v\beta_3$ integrin and moderate affinity for $\alpha_v\beta_5$ integrin is the cyclic pentapeptide c(RGDfV) (*6, 7*). This peptide consists of a head-to-tail cyclic ring containing one D-amino acid and is currently under investigation for tumor imaging and antitumor radiotherapy (*8*).

The present study describes the development of conjugates of the RGD-peptide c(RGDfK) coupled to the side chain amino groups of a protein backbone (Figure 1). Such conjugates have some favorable characteristics that are not present in the parental peptide. For instance, multiple peptide ligands can be attached covalently to the protein. Theoretically, the resulting multivalency of such a conjugate should result in increased avidity for $\alpha_v\beta_3/\alpha_v\beta_5$ integrins. Furthermore, the larger molecular size of such conjugates often results in longer circulation times in the body (*9*). Finally, our goal is to apply RGDpep−protein conjugates as carrier molecules in drug targeting strategies aiming at angiogenic endothelial cells. The larger size of the RGDpep−protein conjugates allows the attachment of multiple drug molecules, instead of the 1:1 coupling ratio of the RGD-4C-doxorubicin construct mentioned above.

In the current study, a series of conjugates were prepared consisting of different amounts of the RGD-peptide c(RGDfK) and a nonrelevant IgG protein backbone. The binding characteristics of such preparations

* To whom correspondence should be addressed. Phone: +31-50-3637627. Fax: +31-50-3633247. E-mail: r.j.kok@farm.rug.nl.

§ Members of UNYPHAR, a network collaboration between the universities of Groningen, Leiden, Utrecht, and the pharmaceutical company Yamanouchi.

‡ Department of Pathology and Laboratory Medicine, Medical Biology section, Tumor Immunology Laboratory.

† Department of Pharmacokinetics and Drug Delivery and Department of Pathology and Laboratory Medicine.

[1] Abbreviations used: RGD-4C, CDCRGDCFC; RGDpep, c(RGDf(ϵ-*S*-acetylthioacetyl)K); RADpep, c(RADf(ϵ-*S*-acetylthioacetyl)K); HuMab, human-anti-mouse antibody; SIA, *N*-succinimidyl iodoacetate; AEC, 3-amino-9-ethylcarbazole; OPD, *o*-phenylenediamine dihydrochloride; GARPO, goat-anti-rabbit-immunoglobulin horseradish peroxidase conjugate; DTDP, 2,2′-dithiodipyridine; mcKLH, mariculture keyhole limpet hemocyanin; PVDF, poly(vinylidene difluoride); HUVEC, human umbilical vein endothelial cells; tTF, truncated Tissue Factor; TNFα, tumor necrosis factor α; IL-2, interleukin-2.

10.1021/bc015561+ CCC: $22.00
Published on Web 12/01/2001

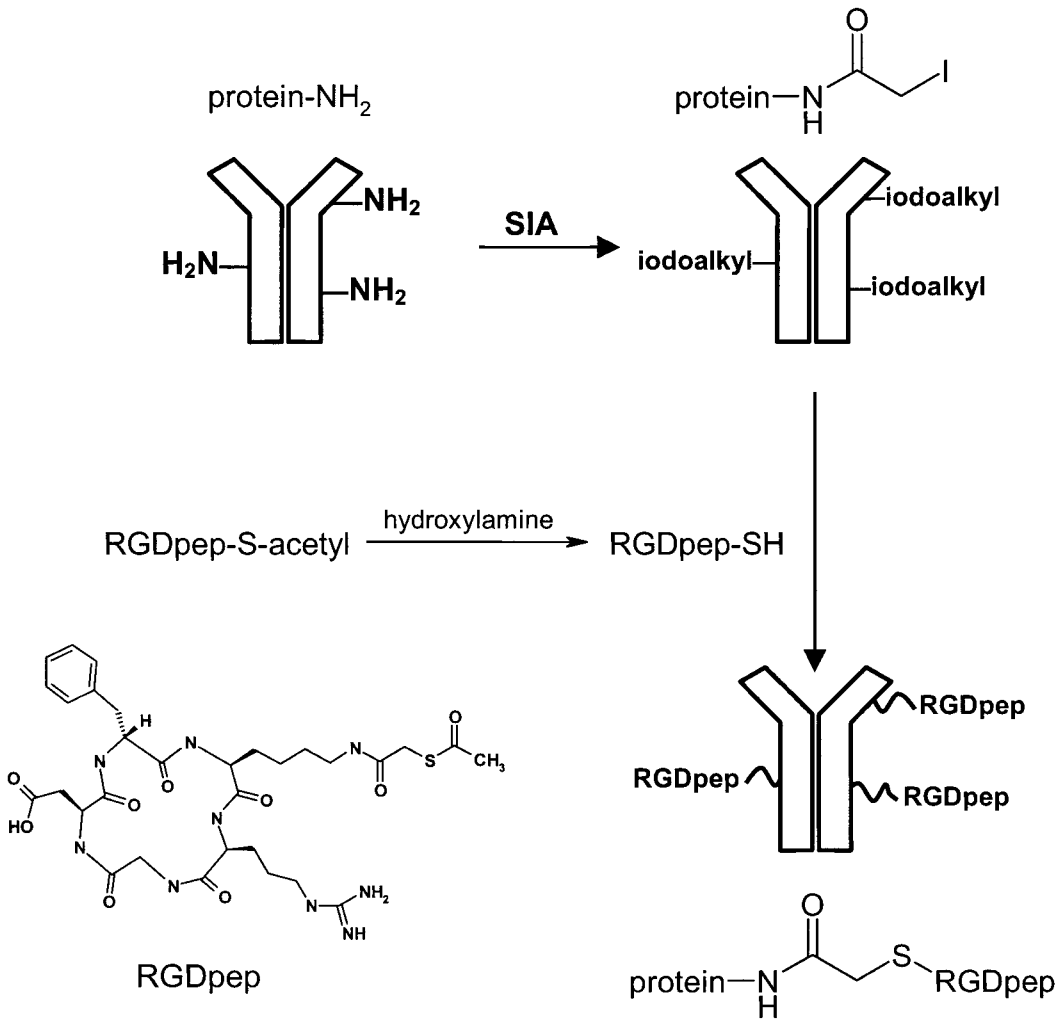

Figure 1. Synthesis of RGDpep−protein conjugates. The iodoacetyl linker (SIA) is coupled to primary amino groups of the protein. After purification by gel filtration, this product is allowed to react in the following reaction. After in situ removal of the protecting thioacetyl group of the peptide with hydroxylamine, RGDpep is coupled via its thiol group with the iodoacetyl group on the protein, resulting in a thioether linkage between RGDpep and protein.

to endothelial cells were studied and compared with those of single monovalent RGD-peptide ligands.

EXPERIMENTAL PROCEDURES

Chemicals and Proteins. All chemicals were used as supplied without further purification. The cyclic RGD-peptide c(RGDf(ϵ-*S*-acetylthioacetyl)K) and the RAD analogue c(RADf(ϵ-*S*-acetylthioacetyl)K), hereafter referred to as RGDpep and RADpep, respectively, were prepared by Ansynth (Roosendaal, The Netherlands). RGD-4C was kindly provided by F. M. H. de Groot (Nijmegen, The Netherlands). c(RGDfV) was obtained from Biomol (Omnilabo International BV, Breda, The Netherlands). HuMab was obtained from the University Hospital Groningen as leftovers from clinical application and consisted of a humanized antibody recognizing an irrelevant human nonendothelial antigen not of interest for our studies. *N*-Succinimidyl iodoacetate (SIA), 3-amino-9-ethyl-carbazole (AEC), *o*-phenylenediamine dihydrochloride tablets (OPD), vitronectin, and crystal violet were obtained from Sigma (St. Louis, MO). 2,2′-Dithiodipyridine (DTDP) was obtained from Fluka (Buchs, Switzerland). L-Cysteine hydrochloride was obtained from Merck (Darmstadt, Germany). Imject Mariculture Keyhole Limpet Hemocyanin (mcKLH), Freund's complete adjuvant, and Freund's incomplete adjuvant were obtained from Pierce (Rockford, IL). Goat-anti-rabbit-peroxidase (GARPO) was obtained from Dako A/S (Glostrup, Denmark). Fibronectin was obtained from Chemicon (Temecula, CA).

Preparation of anti-RGDpep Antiserum. A polyclonal rabbit antiserum was raised against an RGDpep-KLH conjugate in which RGDpep was linked to preactivated mcKLH according to the suppliers protocol. Approximately 600 μg RGDpep-KLH (600 μL) was mixed with an equal volume of Freund's complete adjuvant and injected subcutaneously into a Chinchilla rabbit (Harlan, Zeist, The Netherlands). At 14-day intervals, the immune response was boosted with the injection of RGDpep-KLH emulgated in Freund's incomplete adjuvant (two separate injections of 0.3 mL of emulgate). Blood was collected before immunization and 7 days after immunization. A total of three boosts was needed to obtain adequate anti-RGDpep titers.

Preparation and Characterization of RGDpep−Protein and RADpep−Protein Conjugates. RGDpep or RADpep were coupled in a two-step reaction to the lysine residues in the protein as described below. The iodoacetyl linker molecule SIA was coupled to the primary amino groups of the protein. After purification by size-exclusion chromatography, the SIA-activated proteins were mixed with the peptide and allowed to react after in situ deprotection of the thioacetyl group with hydroxylamine (Figure 1). The peptide:protein ratio of

the conjugate was controlled by varying the amounts of SIA and protein. The peptide was always added in a 2-fold molar excess over the amount of iodoacetyl reagent. To deactivate iodoacetyl groups that had not reacted with the peptide, a final conjugation step was performed with cysteine.

Synthesis of RGDpep−HuMab(I). HuMab (2 mg, 13 nmol) was diluted in PBS to a concentration of 4 mg mL^{-1}. A freshly prepared solution of SIA (19 μg, 67 nmol, 10 mg mL^{-1} in dimethylformamide) was added slowly while the reaction vial was protected from light. The mixture was allowed to react for 1 h at room temperature under gentle mixing. The crude product was purified by sephadex gel filtration (2 serial Hitrap 5 mL desalting columns, Pharmacia Biotech, Roosendaal, The Netherlands) using PBS as eluent at a flow rate of 0.5 mL min^{-1}. The protein-containing fraction was used directly in the following coupling reaction with the peptide. RGDpep (96 μg, 133 nmol), dissolved in an acetonitrile−water mixture (1:4) at a concentration of 10 mg mL^{-1}, was added dropwise to the activated protein. After addition of 100 μL of a freshly prepared hydroxylamine solution (1 M in water), the mixture was allowed to react overnight at room temperature. Remaining iodoacetyl groups were quenched with cysteine (24 μg of hydrochloride salt, 133 nmol, freshly dissolved in water at a concentration of 10 mg mL^{-1}) after which the mixture was reacted for another 1 h. Unreacted reagents were removed by dialysis against PBS at 4 °C. The final product was filtered through a 0.2 μm filter and stored at 4 °C or at −20 °C until further use.

*Synthesis of RGD*pep−Hu*Mab(II)−(IV) and RADpep−HuMab Conjugates.* RGDpep−HuMab and RADpep−HuMab conjugates differing in peptide:protein ratios were prepared according to the same protocol as described above for RGDpep−HuMab(I), using the following amounts of reagents (HuMab/SIA/peptide/cysteine): RGDpep−HuMab(II): 13/133/267/267 nmol; RGDpep−HuMab(III): 13/267/533/533 nmol; RGDpep−HuMab(IV): 13/667/1333/1333; RADpep−HuMab(II): 13/133/267/267 nmol; RADpep−HuMab(IV): 13/667/1333/1333. The amount of hydroxylamine solution (100 μL) was not changed in the various synthesis procedures.

SDS PAGE Analysis and Western Blotting. The covalent coupling of RGDpep or RADpep to the IgG protein in the conjugates was demonstrated by western blotting, followed by immunodetection of coupled peptides in the blotted proteins. For this, the conjugates were subjected to SDS−PAGE analysis performed on a mini-PROTEAN II system (Bio-rad, Veenendaal, The Netherlands) using 7.5% polyacrylamide Tris HCl gels. Samples were prepared for analysis in sample buffer without β-mercaptoethanol (nonreducing conditions) or with β-mercaptoethanol (reducing conditions) to disrupt disulfide bonds between the HuMab IgG subunits. Runned gels were either stained for protein (Coomassie Brilliant Blue staining) or blotted on poly(vinylidene difluoride) membranes (PVDF western blotting membranes, Roche Molecular Biochemicals, Almere, The Netherlands), followed by immunostaining for RGDpep or RADpep using anti-RGDpep polyclonal rabbit antiserum/GARPO/AEC detection. Prestained protein markers (precision prestained molecular weight markers, Bio-rad) were run together with the samples in a separate lane.

Size-Exclusion Chromatography. Molecular size of the prepared conjugates was also analyzed by size-exclusion chromatography under normal conditions, to demonstrate the absence of polymerized IgG or other aggregated proteins due to the conjugation procedures. Separations were performed on a FPLC system equipped with a Superdex 200 HR10/30 column (Pharmacia) and UV detection (214 nm), using PBS at a flow rate of 0.4 mL min^{-1} as mobile phase. HuMab, RGDpep−HuMab(IV), and RADpep−HuMab(IV) conjugates were diluted to a concentration of 100 μg mL^{-1} in PBS, of which 200 μL was injected into the system.

Determination of RGDpep-to-Protein Ratio. The protein content of the conjugates was determined by Lowry (*10*). The number of coupled RGDpep molecules was determined by ELISA using the anti-RGDpep antiserum. Wells were coated with serial dilutions of the RGDpep−protein conjugates for 2 h at 37 °C, washed with 25 mM Tris HCl buffer pH 8 containing 150 mM NaCl and 0.05% Tween 20 and incubated for 1 h with anti-RGDpep antiserum (1:1000 in PBS) at 37 °C, followed by standard detection with GARPO/OPD. The absorbance at 490 nm was measured on a ThermoMax microplate reader (Molecular Devices, Sunnyvale, CA). For each RGDpep−HuMab conjugate, the protein concentration at which 50% of the maximum absorbance was measured (EC_{50}) was calculated by nonlinear regression (Graphpad Prism). The relative RGDpep:protein ratio in each conjugate was calculated by normalization of the EC_{50} to the value of the RGDpep−HuMab(I) conjugate.

An estimate of the absolute RGDpep:protein ratio was obtained by determination of the amount of introduced iodoacetyl groups in the RGDpep−HuMab(IV) conjugate. This number was calculated by reacting the intermediate product SIA−HuMab(IV) with excess cysteine and titration of the remaining amount of free thiol groups with DTDP. In brief, HuMab (13 nmol, 4 mg mL^{-1} in PBS) was reacted with SIA (667 nmol) and purified by gel filtration as described above. To a 1 mL aliquot of the protein-containing fraction were added cysteine (1333 nmol, dissolved in water at a concentration of 10 mg mL^{-1}) and hydroxylamine (100 μL of a freshly prepared 1 M solution in water), and the mixture was stirred for 4 h at room temperature. A 100 μL aliquot was analyzed for thiol content by addition of 900 μL of PBS and 10 μL of DTDP solution (10 mg mL^{-1} in acetone), followed by immediate mixing and measurement of the absorbance at 343 nm. Calibration curves were prepared from a freshly prepared cysteine stock solution. To correct for oxidation of cysteine or consumption of the free thiol other than by reaction with the coupled iodoacetyl groups, a control experiment was performed in which HuMab (13 nmol, 4 mg mL^{-1} in PBS) was *not* reacted with SIA, but otherwise treated similarly as described above. The absolute iodoacetyl:protein ratio of the SIA−HuMab(IV) conjugate was calculated from the decrease in the molar amount of cysteine, corrected for oxidation, and from the protein content of the purified protein.

Cells. Human umbilical vein endothelial cells (HUVEC) were isolated by the method previously described by Mulder (*11*) and cultured on 1% gelatin-precoated plastic tissue culture plates or flasks (Costar Europe, Badhoevedorp, The Netherlands) at 37 °C under 5% CO_2/95% air. The culture medium consisted of RPMI 1640 (BioWittaker, Verviers, Belgium) supplemented with 20% heat-inactivated fetal calf serum (Integro BV, Zaandam, The Netherlands), 2 mM L-glutamine (GIBCO−BRL, Paisley, Scotland), 5 U mL^{-1} heparin (Leo Pharmaceutical Products BV, Weesp, The Netherlands), 100 U mL^{-1} penicillin (Yamanouchi Pharma BV, Leiderdorp, The Netherlands), 100 μg mL^{-1} streptomycin (Radiumfarma-Fisiopharma, Milan, Italy), and 50 μg mL^{-1} endothelial cell growth factor supplement extracted from bovine brain. After attaining confluence, cells were detached

from the surface by trypsin/EDTA (0.5/0.2 mg mL^{-1} in PBS) and split at a 1:3 ratio. HUVEC were used up to passage three.

The H5V mouse endothelioma cell line was kindly provided by Dr. A. Vecchi (Milan, Italy). H5V cells were grown in plastic tissue culture flasks or plates at 37 °C under 5% CO_2/95% air. The culture medium consisted of DMEM supplemented with 10% heat-inactivated FCS, 2 mM L-glutamine, and 300 μg mL^{-1} gentamicin. After attaining confluence, cells were detached from the surface by trypsin/EDTA (0.5/0.2 mg mL^{-1} in PBS) and split at a 1:3 ratio.

Endothelial Cell Adhesion Assay. The functional integrity of the coupled RGDpep was studied in an $\alpha_v\beta_3$-dependent adhesion assay as previously described with minor modifications (*12*). Briefly, flat bottom 96-wells culture plates were coated overnight with vitronectin (500 ng/well in PBS) at 4 °C. Wells were blocked with 1% BSA for 2 h at 37 °C and washed two times with PBS. Trypsinized HUVEC were resuspended in serum-free medium, incubated for 15 min on ice with RGDpep−HuMab or RADpep−HuMab conjugates, and subsequently plated at 2×10^4 cells/well. After incubation at 37 °C for 24 h, unattached cells were removed by rinsing the wells with PBS. Attached cells were fixed in 2% paraformaldehyde, stained with 0.5% crystal violet, and quantified by measuring the absorbance at 575 nm on an Emax microplate reader (Molecular Devices, Sunnyvale, CA). Control experiments included incubations with free RGDpep or RADpep, and adhesion experiments in wells coated with fibronectin, in which case the endothelial cell adhesion is independent of the availability of $\alpha_v\beta_3/\alpha_v\beta_5$ integrins due to adherence via $\alpha_5\beta_1$ integrin. Nonspecific binding of H5V cells was determined by adhesion onto BSA-coated wells.

Radiobinding Assays. The affinity of RGDpep−HuMab conjugates for $\alpha_v\beta_3/\alpha_v\beta_5$ integrin was studied using cells expressing these integrins rather than isolated receptors, to allow cross-linking and possible integrin multimerization in intact cell membranes. RGDpep−HuMab(IV) was radiolabeled with ^{125}I to a specific activity of 0.4 MBq μg^{-1} by a chloramine-T method (*13*). Confluent H5V cell layers in 24-well plates were preincubated for 15 min on ice with binding buffer (50 mM Tris-HCl buffer pH 7.4 supplemented with 150 mM NaCl, 1 mM $CaCl_2$, 1 mM $MgCl_2$, 1mM $MnCl_2$ and 1% BSA). After preincubation, the buffer was replaced by binding buffer containing 70000 cpm of ^{125}I-RGDpep−HuMab(IV) and appropriate dilutions of nonlabeled RGDpep−HuMab conjugates, followed by incubation of the cells for 4 h at 4 °C. After sampling of the supernatant, the cells were washed three times with binding buffer and lysed with 1 M NaOH (30 min at 37 °C). Radioactivity was counted in a LKB multichannel counter (LKB, Bromma, Sweden). Control experiments included competition experiments with RADpep−HuMab conjugates, free RGDpep and RADpep, as well as with c(RGDfV) and RGD-4C.

The K_d of ^{125}I-RGDpep−HuMab(IV) was calculated by nonlinear regression to the Michaelis−Menten equation[2] using the Multifit program (Department of Pharmacokinetics and Drug Delivery, University Centre for Pharmacy, Groningen, The Netherlands). IC_{50} values of RGDpep−HuMab conjugates and RGD-peptides were calculated by nonlinear regression (Graphpad Prism) using a one-site competition model[2].

Statistics. Statistical significance of differences was tested using the two-sided Student's t-test, assuming equal variances.

RESULTS

Preparation and Characterization of Peptide−Protein Conjugates. The peptide RGDpep and its nonbinding counterpart RADpep were coupled covalently to primary amino groups of the HuMab protein after initial derivatization with a iodoacetyl linker (Figure 1). To obtain conjugates with different numbers of coupled peptide, we used ratios of iodoacetyl reagent (SIA) and HuMab of 5:1, 10:1, 20:1, and 50:1 for RGDpep−HuMab-(I) to (IV), respectively. We demonstrated the covalent attachment of RGDpep to HuMab by SDS−PAGE analysis and immunoblotting with a polyclonal anti-RGDpep antiserum (Figure 2). Analysis of samples that were treated with β-mercaptoethanol revealed that the peptide was coupled in both IgG heavy and light chain subunits of the protein. Anti-RGDpep antiserum cross-reacted with RADpep−protein conjugates, but not with conjugates prepared with the iodoacetyl linker and unrelated peptides (data not shown). Therefore, this analysis method could also be applied for the analysis of RADpep−HuMab conjugates.

The covalent conjugation of RGDpep to the HuMab protein was also studied by anti-RGDpep ELISA. This method showed a clear correlation between the RGDpep incorporation and the added equivalents of coupling reagent during the synthesis (Figure 3). From these data, we conclude that we prepared a series of RGDpep−protein conjugates with increasing amounts of coupled RGDpep. In addition, we performed an indirect determination of the number of coupled RGDpep groups for the SIA−HuMab(IV) by reacting the introduced iodoacetyl groups with excess cysteine followed by titration of the remaining free thiol groups with DTDP. This analysis yielded an average of 23 coupled iodoacetyl groups per protein.

Size-exclusion chromatography of the peptide−protein conjugates demonstrated the absence of polymerized protein or other aggregates (Figure 4). A small-increase in molecular size of the conjugates was observed compared to the native IgG protein, both after coupling of RGDpep and RADpep ligands to HuMab.

Endothelial Cell Adhesion Assay. To test the functional integrity of the covalently attached RGDpep, we studied the effect of the RGDpep−HuMab conjugates on the adhesion of endothelial cells on vitronectin-coated surfaces. Figure 5 shows that RGDpep−HuMab conjugates strongly inhibited attachment of HUVEC on vitronectin-coated wells. Similar results were obtained when the adhesion of HUVEC was inhibited by incubation with free RGDpep or with other $\alpha_v\beta_3$ and $\alpha_v\beta_5$ binding peptides such as c(RGDfV) and RGD-4C. In contrast, RADpep−HuMab conjugates had no effect on vitronectin-mediated adhesion. From this, we concluded that the RGDpep−HuMab conjugates functionally interacted with $\alpha_v\beta_3/\alpha_v\beta_5$ in a similar fashion as other RGD-peptide ligands for these integrins. As expected, no inhibition of adhesion by RGDpep−HuMab conjugates was observed in fibronectin-coated wells, which allows HUVEC attachment via both $\alpha_5\beta_1$ and $\alpha_v\beta_3$ integrin (data not shown).

Radiobinding Assays. We studied the binding specificity and affinity of the RGDpep−HuMab conjugates for $\alpha_v\beta_3/\alpha_v\beta_5$-expressing H5V cells with the radioiodinated

[2] One-site binding model: (pmol bound) = $(B_{max})([pM])/(K_d + [pM])$; two-site binding model: (pmol bound) = $(B_{max_1})([pM])/(K_{d_1} + [pM]) + (B_{max_2})([pM])/(K_{d_2} + [pM])$; one-site competition model: % binding = $(100\%)/(1 + 10^{(\log(M) - \log EC_{50})})$.

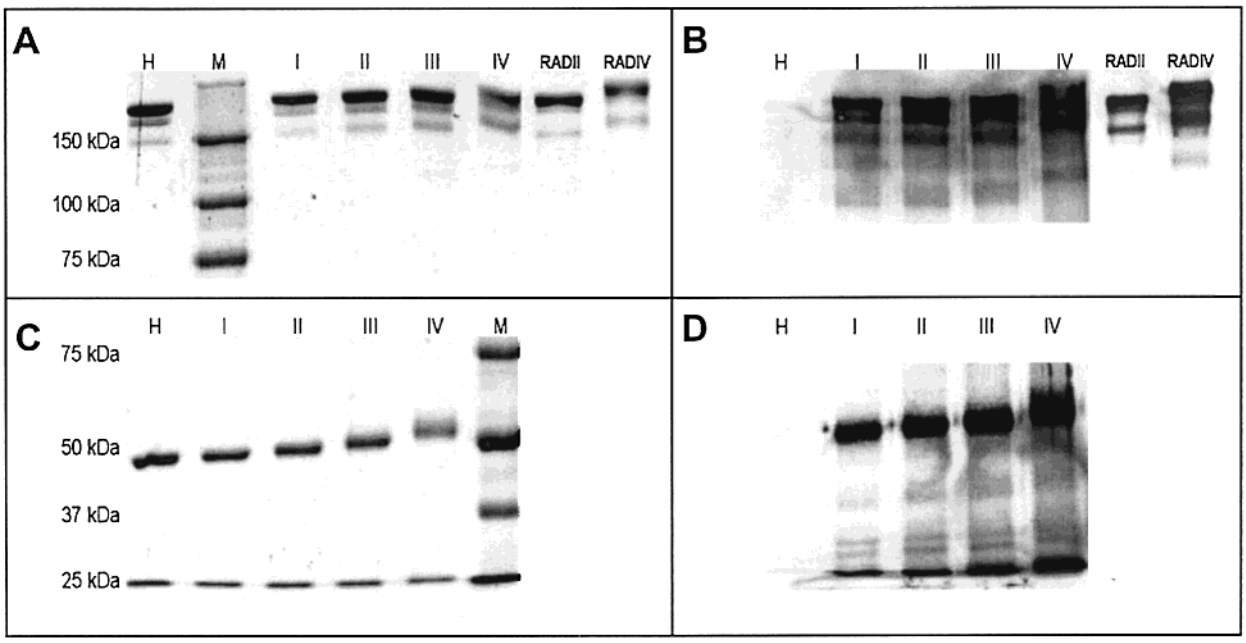

Figure 2. SDS PAGE (A, C) and western blot (B, D) analysis of RGDpep−HuMab conjugates. Panel A: nonreducing conditions, protein staining (Coomassie Brilliant Blue); Panel B: nonreducing conditions, anti-RGDpep immunostaining; Panel C: reducing conditions, protein staining; Panel D: reducing conditions, anti-RGDpep immunostaining. Lanes: (H) HuMab; (M) molecular weight markers; (I to IV) RGDpep−HuMab(I)−(IV); (RADII and -IV) RADpep−HuMab(II) and -(IV).

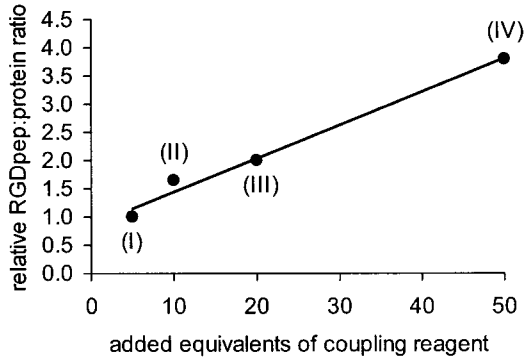

Figure 3. Determination of covalently incorporated RGDpep in RGDpep−HuMab conjugates. Values between parentheses denote the corresponding RGDpep−HuMab conjugate. RGDpep was determined by ELISA using a specific anti-RGDpep antiserum. The relative RGDpep:protein ratio was calculated from the EC_{50} of each conjugate, as determined from the half-maximal OD_{490} absorbance of serial dilutions in the ELISA, and normalized to the value of the RGDpep−HuMab(I) conjugate. See Experimental Procedures for a detailed description of the determination of the relative RGDpep:protein ratio.

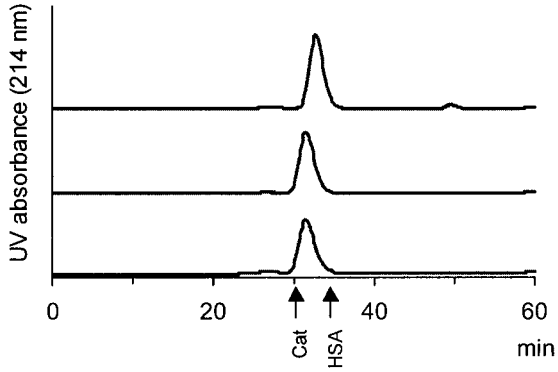

Figure 4. Size-exclusion chromatography of HuMab (upper), RGDpep−HuMab(IV) (middle), and RADpep−HuMab(IV) (bottom). Separations were performed under normal conditions on a Superdex 200 HR10/30 column. Arrows denote the peak elution time of catalase (Cat, 232 kDa) and human serum albumin (HSA, 67 kDa).

RGDpep−HuMab(IV) conjugate. By using whole cells, multivalent binding and clustering of receptors is studied in the natural context of the integrins. The radiobinding experiments were carried out in a Tris binding buffer pH 7.4 supplemented with 1 mM Ca^{2+}, 1mM Mg^{2+}, and 1 mM Mn^{2+}, since these divalent cations are important for the interaction of $\alpha_v\beta_3$ integrin with its ligands (*14*). Experiments in buffers lacking one or more of these cations showed lower absolute binding of ^{125}I-RGDpep−HuMab(IV) (Schraa, A. J., unpublished results).

^{125}I-labeled RGDpep−HuMab(IV) binding could be blocked almost completely by micromolar concentrations of either c(RGDfV) or RGD-4C (Figure 6), indicating that the radiolabeled conjugate bound specifically via its coupled RGDpep groups to the cells. Besides the 50 μM concentration shown in Figure 6, c(RGDfV) at a concentration of 1 M inhibited the binding of ^{125}I-RGDpep−HuMab(IV) to 2.0 ± 0.2% (data not shown).

The specific binding of ^{125}I-RGDpep−HuMab(IV) to the cells was saturable, although maximal binding was not reached at the highest concentration tested (Figure 7). The K_d of RGDpep−HuMab(IV) binding was calculated by nonlinear regression analysis. Assuming two binding sites, which resulted in a better fit of the data than a monovalent model ($p < 0.01$), the analysis yielded binding constants of 0.38 and 22 nM for K1 and K2, respectively (95% confidence intervals: $0.28 < K1 < 0.49$ nM, $0 < K2 < 92$ nM).

We compared the affinities of the RGDpep−HuMab conjugates to the affinity of the parental RGD-peptide by performing competitive displacement studies with the ^{125}I-RGDpep−HuMab(IV) conjugate (Figure 8). All four RGDpep−HuMab conjugates showed a considerable increase in affinity compared to the monovalently binding parental RGD-peptide. Fitting the data with nonlinear regression yielded IC_{50} values presented in Table 1. To compare these data with affinity data of other RGD-peptide ligands, we also determined the IC_{50} of the previously reported c(RGDfV) in our experimental setup

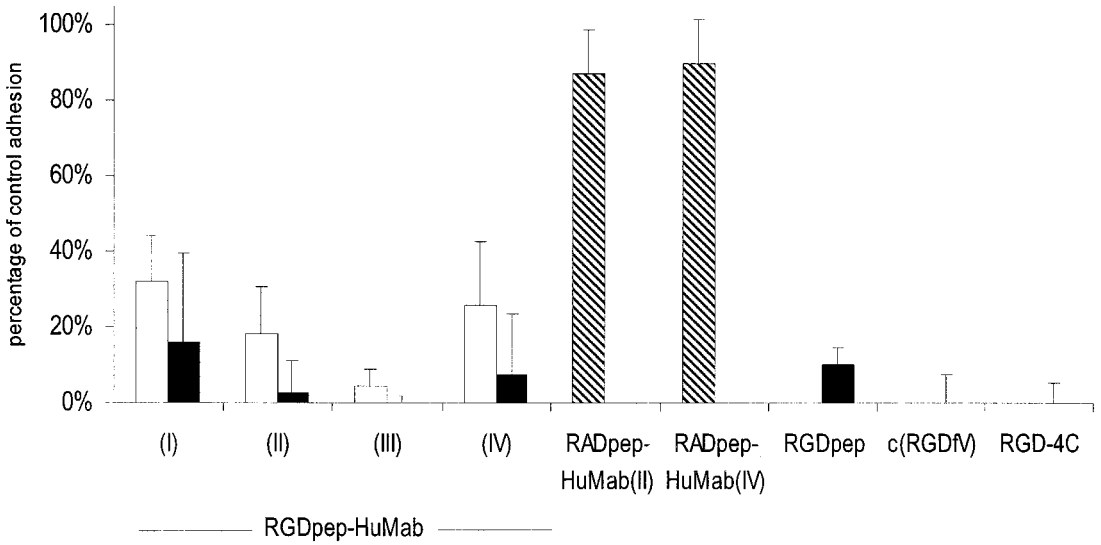

Figure 5. Inhibition of $\alpha_v\beta_3/\alpha_v\beta_5$ mediated adhesion of HUVEC to vitronectin by RGDpep−HuMab conjugates. Adhesion of HUVEC on vitronectin in the absence of inhibitor was set at 100%. Concentration of inhibitors: 500 nM (open bars), 700 nM (hatched bars), 1 μM (closed bars). Values are mean of triplicate assays ± SD. For all RGDpep−HuMab conjugates and RGD-peptides, adhesion of HUVEC significantly differed from control ($p < 0.05$).

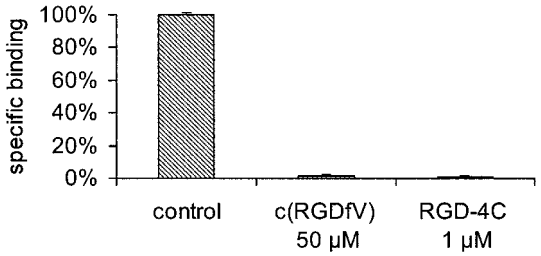

Figure 6. Binding of ^{125}I-RGDpep−HuMab(IV) to H5V endothelial cells. Specific binding of a tracer dose (70000 cpm) of ^{125}I-RGDpep−HuMab(IV) could be inhibited by excess of reported RGD-peptide ligands for $\alpha_v\beta_3/\alpha_v\beta_5$ integrin, c(RGDfV), and RGD-4C. Values are mean of triplicate assays ± SD.

(158 nM). The RGDpep used for preparation of our constructs, c(RGDf(ϵ-*S*-acetylthioacetyl)K), competed at a 5-fold higher IC_{50} than c(RGDfV), likely resulting from the attachment of the acetylthioacetyl linker group.

Competition experiments with RADpep and RADpep−HuMab conjugates showed no inhibition of ^{125}I-RGDpep−HuMab(IV) binding, even at the highest concentration tested. Again, this demonstrates that the binding of ^{125}I-RGDpep−HuMab(IV) is specifically mediated via the coupled RGDpep groups.

DISCUSSION

The present study describes the preparation and characterization of multivalent derivatives of a peptide that binds to $\alpha_v\beta_3$ and $\alpha_v\beta_5$ integrins via an Arg-Gly-Asp sequence. We coupled this RGDpep chemically to a protein and demonstrated that such RGDpep−protein conjugates bind to endothelial cells with dramatically increased affinity. Since the binding of the RGDpep−protein conjugates can be inhibited by the free RGDpep and other RGD-peptides, but not by similarly prepared RADpep−protein conjugates, we concluded that RGDpep−protein conjugates bind to the cells via the coupled RGDpep groups.

The type of RGD-peptide that was used in the present study binds specifically and with high affinity to $\alpha_v\beta_3$ integrin due to the special constrained conformation of the RGD sequence (*6*). This special RGD conformation is induced by both the unnatural D-amino acid and the head-to-tail cyclization of the pentapeptide. Since such peptide structures cannot be encoded by a recombinant DNA sequence, we have chosen for classical chemical coupling techniques to prepare RGDpep−protein derivatives. In these conjugates, the peptide was coupled via a relatively short linker to amino groups of the HuMab

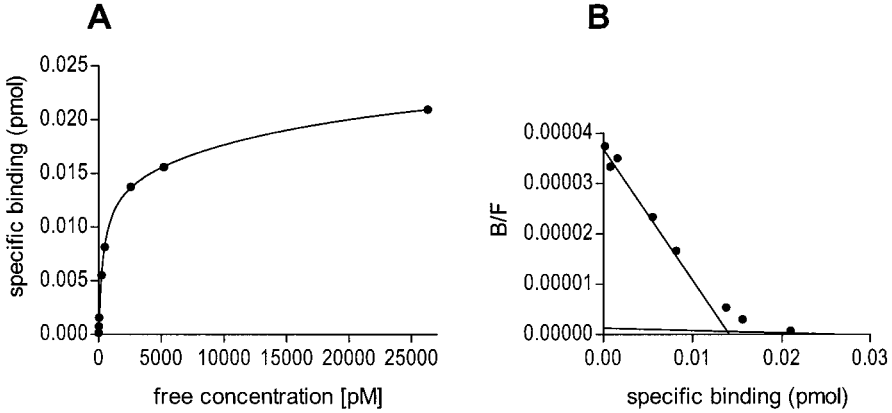

Figure 7. Specific binding of ^{125}I-RGDpep−HuMab(IV) to H5V endothelial cells after incubation for 4 h at 4 °C. Panel A: Specific binding of ^{125}I-RGDpep−HuMab(IV) (pmol/well) plotted against the free concentration of the compound [pM]. Panel B: Scatchard plot of ^{125}I-RGDpep−HuMab(IV) binding. B/F: ratio of specific binding and free concentration (pmol/pM). Fitted lines in both panels were drawn using the K_d and B_{max} values calculated by nonlinear regression analysis.

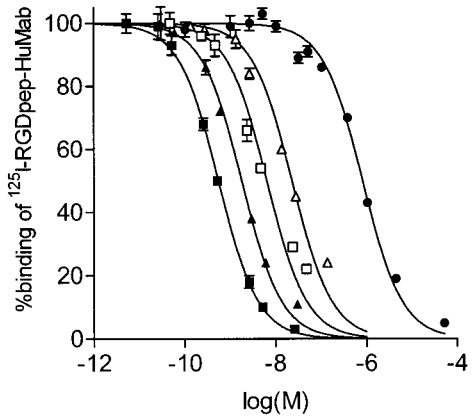

Figure 8. Competitive displacement of ^{125}I-RGDpep−HuMab-(IV) binding by RGDpep−HuMab conjugates and parental RGDpep. H5V cells were incubated with ^{125}I-RGDpep−HuMab-(IV) (tracer dose, 70000 cpm) and appropriate dilutions of nonlabeled compounds. Cell-associated radioactivity in the absence of competitor was set at 100%. Closed circles: RGDpep; open triangles: RGDpep−HuMab(I); open squares: RGDpep−HuMab(II); closed triangles: RGDpep−HuMab(III); closed squares: RGDpep−HuMab(IV). Values are mean of triplicate assays ± SD.

Table 1. Affinity Data of RGDpep−HuMab Conjugates and RGD-Peptides. Competitive Binding Experiments Were Performed on $\alpha_v\beta_3$ Integrin Expressing H5V Cells with Radiolabeled RGDpep−HuMab(IV) Conjugate and the Peptide−Protein Conjugates or Peptides Products Listed below. IC_{50} Values Were Calculated from the Data Presented in Figure 8

product	IC_{50} (nM)	increase in affinity[a]
RADpep	>5000[b]	
RGDpep	818	1
c(RGDfV)	158	5
RGDpep−HuMab(I)	23.2	35
RGDpep−HuMab(II)	6.5	125
RGDpep−HuMab(III)	2.0	410
RGDpep−HuMab(IV)	0.6	1297
RADpep−HuMab(II)	>667[b]	
RADpep−HuMab(IV)	>667[b]	

[a] The increase in affinity was calculated by dividing the IC_{50} of RGDpep by the IC_{50} of the tested product. [b] Highest tested concentration. No inhibition of ^{125}I−RGDpep−HuMab(IV) binding was observed at this concentration.

protein. Since the RGD-binding site of integrins is located in a cleft between the two subunits of the integrin, the pharmacological activity of RGD-peptide could be lost due to steric hindrance of the protein backbone. The spacer in our conjugates accounts for 10 atoms, counted from protein backbone to the ϵ-amino group of the lysine in the c(RGDfK) ring structure. This value fits in the spacer requirements found by Kantlehner and colleagues, who demonstrated that c(RGDfK) coupled via an 8-atom spacer lost its activity, while a 15-atom spacer allowed the peptide to interact freely with its receptor (*15*). Clearly, the binding of our conjugates to endothelial cells and the inhibition of adhesion of HUVEC onto vitronectin-coated wells demonstrate the functional activity of our constructs with $\alpha_v\beta_3$ integrin.

We determined the amount of coupled RGDpep ligands in our conjugates by an anti-RGDpep ELISA, which enabled us to calculate relative RGDpep:protein ratios ranging from 1 to 3.8. In addition, we determined the amount of introduced iodoacetyl groups of the SIA−HuMab(IV) conjugate. From this experiment an absolute RGDpep:protein ratio for the RGDpep−HuMab(IV) conjugate of 23 was established. Since the RGDpep−HuMab-(I) conjugate was prepared using 5 equiv of SIA reagent, the maximal amount of coupled RGDpep molecules in the RGDpep−HuMab(IV) conjugate based on the ELISA would be 19, which is lower than the absolute ratio of 23. Likely, the observed discrepancy results from an underestimation of the relative RGDpep:protein ratio, due to steric hindrance of anti-RGDpep antibody binding in the higher loaded conjugates.

Commonly, the degree of protein modification is calculated indirectly, for instance by TNBS derivatization of remaining primary amino groups (*16*). This approach proved to be inaccurate for our conjugates, due to the low protein concentration of the products. Alternatively, the number of coupled peptides can be derived from the change in apparent molecular weight demonstrated by gel electrophoresis or chromatography (*17*). However, our products showed only small differences compared to the parent protein, probably due to the constrained structure of the RGDpep ligand, although immunostaining clearly demonstrated the presence of the peptide in all conjugates. The large molecular weight of HuMab and the expected heterogeneity of the conjugates would furthermore not allow proper mass spectrometry analysis of the conjugates.

We studied the affinity of our conjugates for cells expressing $\alpha_v\beta_3/\alpha_v\beta_5$ integrins using the radiolabeled RGDpep−HuMab(IV) conjugate, which contained the highest number of coupled RGDpep ligands. ^{125}I-RGDpep−HuMab(IV) bound in a saturable manner to these endothelial cells, although complete saturation of binding was not observed at highest concentration tested. Assuming two binding sites in the fitting model gave better results than a one-binding site model. Whether the conjugate actually binds via two RGDpep-integrin interactions cannot be concluded from our data. More likely, the found binding constants are apparent K_d values.

To compare the binding affinities of the RGDpep−HuMab conjugates with those of free RGDpep and references from the literature, we determined the IC_{50} values of the various RGD-containing compounds (Table 1). The increase in IC_{50} correlated with the number of coupled RGDpep groups for the series of RGDpep−HuMab conjugates. Since the affinity increased to a larger extent than can be accounted for by the number of coupled RGDpep ligands, only cooperative binding due to multivalency can explain these data. Compared to the single RGDpep ligand, an increase in IC_{50} was found of over 3 orders of magnitude for the most potent RGDpep−HuMab conjugate, while about 23 RGDpep ligands have been incorporated in this product. Compared to the reference c(RGDfV), an increase in affinity of up to 250-times was calculated for the RGD-HuMab(IV) product. In comparison, the most potent structure derived from c(RGDfV), c(RGDf(N-Me)V) (EMD121974), binds to $\alpha_v\beta_3$ with an affinity 4.3 times higher than c(RGDfV) (*18*).

To summarize, the coupling of the peptide RGDpep to a protein yielded multivalent conjugates with a strongly increased affinity for $\alpha_v\beta_3$ integrin and/or $\alpha_v\beta_5$ integrin compared the parental peptide. These conjugates were capable of inhibiting the interaction between $\alpha_v\beta_3/\alpha_v\beta_5$ integrins and vitronectin and therefore may display antiangiogenic effects when administered in vivo. In addition, RGDpep-conjugation might be of use for targeting of therapeutic proteins to tumor blood vessels. Candidate proteins for such an approach currently under investigation in our laboratory include truncated Tissue Factor (tTF), that selectively induces blood coagulation in tumor blood vessels when properly bound to receptors on the tumor endothelium (*19*). Initial experiments with RGDpep-tTF conjugates demonstrated that RGDpep-tTF

was still capable of inducing blood coagulation in vitro (Schraa, A. J., unpublished results). Alternatively, RGDpep−protein conjugates can be prepared that induce tumor endothelial cell killing. Examples of proteins that can be used in the latter approach are TNFα and IL-2, both activating the immune system, or glucose oxidase, which generates toxic reactive oxygen species (*20*−*22*). Finally, endothelial delivery of small drug molecules or toxic molecules can be achieved using RGDpep as a targeting device. The validity of such an approach has already been demonstrated with the RGD-4C−doxorubicin prodrug, which displayed a strong antitumor effect (*4*). Preparations based on this approach can either consist of soluble macromolecules, such as proteins or polymeric backbones, or liposomal formulations as recently proposed by Kessler et al. (*23*, *24*).

ACKNOWLEDGMENT

A.D. Berendsen is kindly acknowledged for assisting in the radiobinding experiments, and J.H. Pol from the Department of Nuclear Medicine for radiolabeling of the conjugates. HUVEC and H5V cells were kindly provided by the RuG/AZG Endothelial Cell Facility.

LITERATURE CITED

(1) Griffioen, A. W., and Molema, G. (2000) Angiogenesis: potentials for pharmacologic intervention in the treatment of cancer, cardiovascular diseases, and chronic inflammation. *Pharmacol. Rev. 52* (*2*), 237−268.

(2) Ruoslahti, E., and Rajotte, D. (2000) An address system in the vasculature of normal tissues and tumors. *Annu. Rev. Immunol. 18*, 813−827.

(3) Koivunen, E., Wang, B., and Ruoslahti, E. (1995) Phage libraries displaying cyclic peptides with different ring sizes: ligand specificities of the RGD-directed integrins. *Biotechnology (N. Y.) 13* (*3*), 265−270.

(4) Arap, W., Pasqualini, R., and Ruoslahti, E. (1998) Cancer treatment by targeted drug delivery to tumor vasculature in a mouse model. *Science 279* (*5349*), 377−380.

(5) Assa-Munt, N., Jia, X., Laakkonen, P., and Ruoslahti, E. (2001) Solution structures and integrin binding activities of an RGD peptide with two isomers. *Biochemistry 40* (*8*), 2373−2378.

(6) Haubner, R., Gratias, R., Diefenbach, B., Goodman, S. L., Jonczyk, A., and Kessler, H. (1996) Structural and functional aspects of RGD-containing cyclic pentapeptides as highly potent and selective integrin alpha-v-beta-3 antagonists. *J. Am. Chem. Soc. 118*, 7461−7472.

(7) Lohof, E., Planker, E., Mang, C., Burkhart, F., Dechantsreiter, M. A., Haubner, R., Wester, H. J., Schwaiger, M., Holzemann, G., Goodman, S. L., and Kessler, H. (2000) Carbohydrate Derivatives for Use in Drug Design: Cyclic alpha(v)-Selective RGD Peptides. *Angew. Chem., Int. Ed. 39* (*15*), 2761−2764.

(8) Haubner, R., Wester, H. J., Reuning, U., Senekowitsch-Schmidtke, R., Diefenbach, B., Kessler, H., Stocklin, G., and Schwaiger, M. (1999) Radiolabeled alpha(v)beta3 integrin antagonists: a new class of tracers for tumor targeting. *J. Nucl. Med. 40* (*6*), 1061−1071.

(9) Meijer, D. K. F., and Ziegler, K. (1993) Mechanisms for the hepatic clearance of oligopeptides and proteins. Implications for rate of elimination, bioavailability and cell-specific drug delivery to the liver. *Biological Barriers to Protein Delivery* (K. L. Audus, T. J. Raub, Eds.) pp 339−408, Plenum Press, New York.

(10) Lowry, O. H., Rosebrough, N. J., Farr, A. L., and Randall, R. J. (1951) Protein measurement with the Folin Phenol reagent. *J. Biol. Chem. 193*, 265−275.

(11) Mulder, A. B., Blom, N. R., Smit, J. W., Ruiters, M. H., van der, M. J., Halie, M. R., and Bom, V. J. (1995) Basal tissue factor expression in endothelial cell cultures is caused by contaminating smooth muscle cells. Reduction by using chymotrypsin instead of collagenase. *Thromb. Res. 80* (*5*), 399−411.

(12) Ruegg, C., Yilmaz, A., Bieler, G., Bamat, J., Chaubert, P., and Lejeune, F. J. (1998) Evidence for the involvement of endothelial cell integrin alphaVbeta3 in the disruption of the tumor vasculature induced by TNF and IFN-gamma. *Nat. Med. 4* (*4*), 408−414.

(13) Hunter, W. M., and Greenwood, F. C. (1962) Preparation of iodine-131 labeled human growth hormone of high specific activity. *Nature 194* (*4827*), 495−496.

(14) Legler, D. F., Wiedle, G., Ross, F. P., and Imhof, B. A. (2001) Superactivation of integrin alphavbeta3 by low antagonist concentrations. *J. Cell Sci. 114* (*Pt 8*), 1545−1553.

(15) Kantlehner, M., Finsinger, D., Meyer, J., Schaffner, P., Jonczyk, A., Diefenbach, B., Nies, B. and Kessler, H. (1999) Selective RGD-mediated adhesion of osteoblasts at surfaces of implants. *Angew. Chem., Int. Ed. 38* (*4*), 560−562.

(16) Habeeb, A. F. S. A. (1966) Determination of free amino groups in proteins by trinitrobenzenesulfonic acid. *Anal. Biochem. 14*, 328−336.

(17) Beljaars, L., Molema, G., Schuppan, D., Geerts, A., De Bleser, P. J., Weert, B., Meijer, D. K. F., and Poelstra, K. (2000) Successful targeting of albumin to rat hepatic stellate cells using albumin modified with cyclic peptides that recognize the collagen type VI receptor. *J. Biol Chem. 275* (*17*), 12743−12751.

(18) Dechantsreiter, M. A., Planker, E., Matha, B., Lohof, E., Holzemann, G., Jonczyk, A., Goodman, S. L., and Kessler, H. (1999) *N*-Methylated cyclic RGD peptides as highly active and selective alpha(V)beta(3) integrin antagonists. *J. Med. Chem. 42* (*16*), 3033−3040.

(19) Huang, X., Molema, G., King, S., Watkins, L., Edgington, T. S., and Thorpe, P. E. (1997) Tumor infarction in mice by antibody-directed targeting of tissue factor to tumor vasculature. *Science 275* (*5299*), 547−550.

(20) Curnis, F., Sacchi, A., Borgna, L., Magni, F., Gasparri, A., and Corti, A. (2000) Enhancement of tumor necrosis factor alpha antitumor immunotherapeutic properties by targeted delivery to aminopeptidase N (CD13). *Nat. Biotechnol. 18* (*11*), 1185−1190.

(21) Lode, H. N., Moehler, T., Xiang, R., Jonczyk, A., Gillies, S. D., Cheresh, D. A., and Reisfeld, R. A. (1999) Synergy between an antiangiogenic integrin alphav antagonist and an antibody-cytokine fusion protein eradicates spontaneous tumor metastases. *Proc. Natl. Acad. Sci. U.S.A. 96* (*4*), 1591−1596.

(22) Christofidou-Solomidou, M., Pietra, G. G., Solomides, C. C., Arguiris, E., Harshaw, D., FitzGerald, G. A., Albelda, S. M., and Muzykantov, V. R. (2000) Immunotargeting of glucose oxidase to endothelium in vivo causes oxidative vascular injury in the lungs. *Am. J. Physiol. Lung Cell. Mol. Physiol. 278* (*4*), L794-L805.

(23) Kok, R. J., Asgeirsdottir, S. A., and Verweij, W. R. (2001) Development of proteinaceous drug targeting constructs using chemical and recombinant DNA approaches. *Drug targeting: organ-specific strategies* (G. Molema, D. K. F. Meijer, Eds.) pp 275−308, Wiley-VCH, Weinheim, Germany.

(24) Marchi-Artzner, V., Lorz, B., Hellerer, U., Kantlehner, M., Kessler, H. and Sackmann, E. (2001) Selective adhesion of endothelial cells to artificial membranes with a synthetic RGD-lipopeptide. *Chemistry 7* (*5*), 1095−1101.